# Binding of Chitosan to Phospholipid Vesicles Studied with Isothermal Titration Calorimetry

Omar Mertins* and Rumiana Dimova*

Department of Theory and Bio-Systems, Max Planck Institute of Colloids and Interfaces, Science Park Golm, 14424 Potsdam, Germany

ABSTRACT: We thermodynamically characterize the interaction of chitosan with small liposomes and the binding and organization of the polysaccharide on the membrane of the vesicles. By means of isothermal titration calorimetry (ITC), we obtain the enthalpy variations arising from binding of the positively ionized chitosan to neutral and negatively charged liposomes. The strong electrostatic interaction of the polysaccharide with the negative charges at the membrane gives rise to highly exothermic signal until charge compensation is reached. The equilibrium constant, the interaction stoichiometry, and the molar enthalpy of binding chitosan monomers to phospholipids from the external leaflet of the vesicle membrane are obtained from the isotherm curve fitting assuming independent binding sites. The strong exothermic signal indicates that the electrostatically driven binding of chitosan to the membrane is energetically favored, leading to further stabilization of the vesicle suspension. The higher the net negative charge of the vesicles, the more pronounced the adsorption of chitosan is, leading to weaker chain organization of the adsorbed chitosan at the membrane. At the point of charge saturation, vesicle aggregation takes place and we show that this behavior does not always lead to charge reversal at the membrane. Models for the binding behavior and structural organization of chitosan are proposed based on the experimental results from ITC, ζ-potential, and dynamic light scattering.
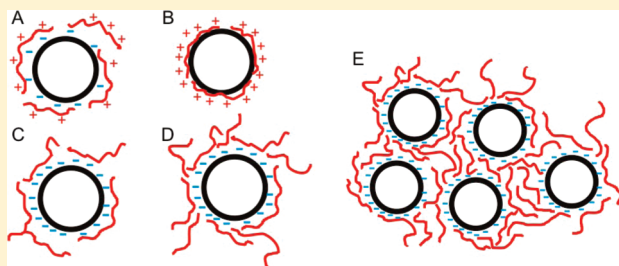
1. INTRODUCTION

Liposomes are colloidal structures where phospholipids self-assemble to form the membrane of small spheres encapsulating polar liquids. Described for the first time more than 40 years ago,[1] liposomes have found a large spectrum of applications in particular as drug delivery systems.[2,3] The directions in developing such systems follow the concept of drug targeting with sensibly reduced side effects as well as optimization of the treatment. The projection of a developed drug vector relies on increased circulation time and specificity of targeting. To fulfill such requirements, liposomes have been modified and adapted to the environment of application, thus achieving higher performance. For instance, well established and widely employed are stealth liposomes,[2] where the decoration of the vesicle membrane with polyethylene glycol leads to an increase of the circulation time of the vesicles, because the clearance by macrophage cells in the human bloodstream is avoided.[4] The successful use of polyethylene glycol also opened the path for implementation of other macromolecules to improve the liposome characteristics. The use of natural polymers has received special attention. Among them, chitosan has shown some advantages. Chitosan is an α-(1→4)-2-amino-2-deoxy-β-D-glucan polysaccharide (see Figure 1A) obtained by partial deacethylation of chitin.[5] It is known as a biocompatible and biodegradable polymer. Liposomes modified with chitosan have shown applicability in particular for drug delivery in the gastrointestinal tract,[6] since the polymer improves the stability of vesicles in different pH conditions.[7]

In order to optimize the formation process of liposomes decorated with chitosan (chitosomes), one has to consider the physical properties of the polymer as well as its interactions with the membrane. Chitosan is typically water-soluble at pH under 5.5[8] due to ionization of the amino groups in the repeat unit of the polymer chain. Therefore, in the preparation of chitosomes, one may take advantage of the electrostatic interactions between the positive amino groups of chitosan and the negative charges at the polar heads of phospholipids. The presence of the polymer at the vesicle membrane modifies the properties of liposomes. Recent reports have shown that chitosan may change the structural parameters of liposome suspensions[9−11] and increase the phase transition temperature of the phospholipid bilayer, leading to higher thermal stability.[12] The distribution of the polymer at the membrane of model giant liposomes has also been studied and quantified[13,14] and the effective interaction of the polymer with the phosphate group of phosphatidylcholine was determined by ^{31}P NMR spectroscopy.[15] Not only electrostatic interactions have been considered in the literature. Depending on the chitosome preparation method, different organization of the macromolecules on the vesicles is observed, suggesting that different types of interactions may be involved. For instance, Fang et al. have shown that hydrophobic interactions between the phospholipid apolar tails and the polymer backbone may be
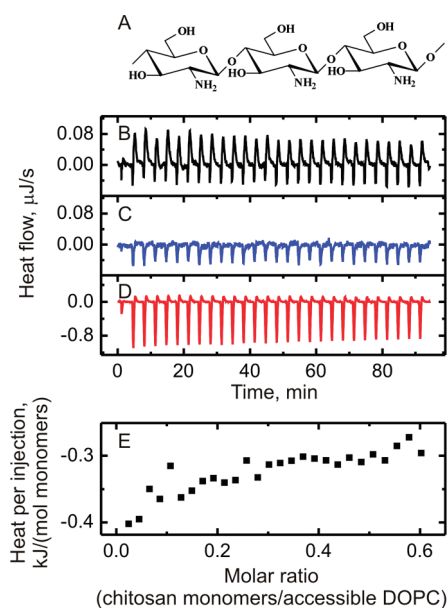
Figure 1. Molecular structure of idealized chitosan (A). Isothermal titration calorimetry data for the dilution of chitosan solution with 6.13 mM monomer concentration (95% DDA, 199 kDa) in buffer (B), titration of chitosan-free buffer into suspension of DOPC liposomes with 3.82 mM lipid concentration (C), titration of the chitosan solution in the liposome suspension (D, E). Panels B−D show heat flows, while panel E presents the integrated heat per injection versus the molar ratio of chitosan monomers to DOPC in the external leaflet of liposomes. The data in panel E were corrected for dilution effects by subtracting the data for chitosan dilution. Both the chitosan and the vesicle solutions were prepared in 80 mM acetate buffer at pH 4.48. All measurements were performed at 25 °C.

increased when premixing both molecules in an organic solvent before vesicles self-assemble.[16] More recently, we have shown that a modification of the method of electroformation of giant vesicles, based on an inverse phase precursor emulsion, allows the introduction of macromolecules like chitosan.[13] With this approach the production process promotes strong physical adsorption and deposition of chitosan on both sides of the membrane, whereby possible hydrophobic interactions may be involved. Pavinatto et al. have also shown interesting results with Langmuir monolayers, concluding that even though electrostatic interactions may be the main energy contribution in the chitosan−phospholipid couple, other secondary interactions may also play a certain role.[17] Apart from hydrophobic interactions, effects arising from hydrogen bonding and van der Waals forces have also been considered in the literature.[18,19]

Despite of the relatively large number of studies on the adsorption of chitosan on liposomes, thermodynamic characteristics of the binding process have not been provided so far. Usually vesicles are prepared, ζ-potential is measured before and after chitosan addition, and the interpretation is limited mainly to surface charge modifications.[14,20−23] In the present work, we aim to extend the available biophysical studies by thermodynamically characterizing the interactions involved in the encounter of chitosan with small unilamellar liposomes leading to the binding and organization of the polysaccharide at the membrane of the vesicles.

Here, for the first time we employ isothermal titration calorimetry (ITC) for the detailed thermodynamic characterization of the

binding of chitosan to neutral and charged liposomes. Previously, ITC has been used with neutral phosphocholine vesicles and only qualitative description of the process was reported.[14] In our study, we explore vesicles with varied surface charge, deduce the binding stoichiometry, extract the molar enthalpy, and characterize the entropic contributions involved. The link between our ITC results and data from established methods is then made using traditional ζ-potential and dynamic light scattering (DLS) measurements in parallel. The thermodynamic characteristics of the predominant electrostatic interactions are quantified, secondary effects that may influence the interactions are discussed, and models of binding behavior and structural organization of chitosomes and of the polymer at the membrane are proposed on the basis of the experimental data.

2. MATERIALS AND METHODS

2.1. Materials. Chloroform solutions of 1,2-dioleoyl-*sn*-glycero-3-phosphatidylcholine (DOPC) and 1,2-dioleoyl-*sn*-glycero-3-phosphatidylglycerol (sodium salt) (DOPG) were purchased from Avanti Polar Lipids Inc. (Birmingham, AL) and used without further purification. The choice for DOPC as the lipid for vesicle preparation is based on the fact that this is the lipid employed in previous studies,[13,14,21] to which comparison of the present results could be made. As a source for negative surface charge on the membrane, we employed DOPG because it has the same hydrophobic moiety as DOPC. The lipids were stored at −20 °C upon arrival. Chitosan was a gift from Primex, with 95% degree of deacetylation (DDA). The average molecular weight was determined as M_w = 199 kDa (corresponding to 1223 repeat monomers per molecule) using multiangle laser light scattering−size exclusion chromatography (MALLS−SEC),[24] with a radius of gyration of 46 nm and refractive index increment dn/dc = 0.203 mL/g. All other reagents were of analytical grade. All solutions were prepared using deionized water from Milli-Q Millipore system with a total organic carbon value of less than 15 ppb and a resistivity of 18 Ω cm.

2.2. Preparation of Liposomes and Chitosan Solutions. The lipid solutions in chloroform were transferred into round-bottom flasks and the organic solvent was removed by evaporation using a nitrogen gas stream until completely dried followed by 2 h of vacuum pumping. The lipid film was then dissolved in an aqueous buffer solution of acetic acid/sodium acetate. The buffer was prepared at a total concentration of 80 mM to obtain the desired pH 4.48 with a maximal variation of 0.01. Liposomes were obtained by vortexing for about 2 min followed by extrusion using a LipsosoFast pneumatic extruder (Avestin Inc., Ottawa, Canada) operating at a pressure of 200 kPa. The final total lipid concentration for all experiments was 3.82 mM and the proportion between DOPC and DOPG was varied to obtain neutral vesicles made of pure (100%) DOPC or negatively charged vesicles with 10, 20, 30, or 40% DOPG (corresponding to 0.38, 0.76, 1.15, and 1.53 mM DOPG, respectively). The extrusion was performed in three consecutive stages, 20 times through a 400 nm diameter pore polycarbonate filter, 20 times through a 200 nm diameter pore filter, and finally 40 times through a 100 nm diameter pore filter. Vesicles prepared in this way generally have a narrow size distribution, as confirmed with dynamic light scattering, and are known to be almost entirely unilamellar.[25]

The chitosan solution was prepared by vigorous overnight stirring of the powder in the same acetate buffer (pH 4.48 ± 0.01), at a concentration of 1 mg/mL corresponding to 6.13 mM of monomers. Solutions with lower concentrations were prepared by diluting the stock solution with buffer.

The pH of all solutions was always monitored before and after sample preparation, and the conductivity was measured, to ensure constant ionic strength. Acetic acid was added to adjust the pH when required.

2.3. Dynamic Light Scattering and ζ-Potential. Size distribution measurements were performed with a Malvern Zetasizer 300 ZS (Malvern Instruments) operating with a 2 mW HeNe laser at a wavelength of 632.8 nm and detection at an angle of 173°. All measurements were performed in a temperature-controlled chamber at 25 °C. The autocorrelation function was acquired using exponential spacing of the correlation time. The data analyses were performed with software provided by Malvern. The intensity-weighted size distribution was obtained by fitting data with a discrete Laplace inversion routine.[26]

The ζ-potential of vesicles and chitosan was measured with the same Malvern Zetasizer performing at least six runs per sample. The measurement principle is based on laser Doppler velocimetry. The mobility u is converted to the ζ-potential using the Helmholtz–Smoluchowski relation, $\zeta = u\eta/\varepsilon\varepsilon_0$, where η is the solution viscosity, ε the dielectric constant of water, and ε_0 the permittivity of free space.

2.4. Isothermal Titration Calorimetry. ITC measurements were performed with VP-ITC microcalorimeter from MicroCal Inc. (Northampton, MA). The working cell (1.442 mL in volume) was typically filled with the liposome suspension and the reference cell with the corresponding liposome-free buffer solution. One aliquot of 2 μL followed by 27 aliquots of 10 μL of chitosan solution (pH 4.48 ± 0.01) were injected stepwise with 200 s interval into the working cell filled with the vesicle suspension. The corresponding reference blank experiments were also performed, namely titration of chitosan-free buffer in the vesicle suspension and titration of chitosan solution in vesicle-free buffer. The inverse experiments, meaning titration of vesicle suspension into chitosan solution, were also performed for the neutral vesicles. To avoid the presence of bubbles, all samples were degassed for 10 min shortly before starting the measurements. The sample cell was constantly stirred at a rate of 307 rpm, and the measurements were performed at 25 °C. The data analyses were carried out with Origin software provided by MicroCal.

3. RESULTS AND DISCUSSIONS

3.1. Binding of Chitosan to Neutral Phosphocholine Vesicles. Figure 1B shows the heat flow associated with the stepwise dilution of chitosan solution at a concentration of 1 mg/mL (6.13 mM monomeric concentration). Each injection of the chitosan solution in the same chitosan-free buffer solution produces a very weak exothermic (downward pointing) peak immediately followed by a small endothermic (upward pointing) peak of similar magnitude. The overall heat associated with one injection is positive, i.e. endothermic, and corresponds to an average of 0.57 μcal/injection or 9.2 cal/mol of injected chitosan monomers. Presumably, the exothermic part of the signal in Figure 1B is related to dilution when chitosan is transferred from a highly concentrated solution to a low-concentration one (or to chitosan-free solution for the first injection). The endothermic part may be the result of the molecular reorganization of chitosan in the highly diluted solution under stirring. Note that since both effects are very small, they denote the exceptional sensitivity of the technique and show that chitosan properties like the degree of ionization of the amino groups are not being modified in the dilution process, at least in the concentration range applied in this titration. However, an important condition for the success of these measurements is that the pH of the chitosan solution must be exactly the same as that of the buffer in the reaction cell to avoid contributions resulting from pH change during the injections. Even very slight differences in pH were found to give high enthalpic effect (data not shown). For this reason, the pH of all solutions was always controlled and adjusted to 4.48 ± 0.01 with

acetic acid when required (see Materials and Methods for details).

The second reference measurement, titration of buffer in the suspension of neutral liposomes, gives also small heats of dilution, −0.28 μcal/injection on average (see Figure 1C). In this case, there is a negligible exothermic effect as a result of dilution of liposomes.

Titration of the chitosan solution into the suspension of neutral vesicles gives the heat release, as shown in Figure 1D. Similar to chitosan dilution, there is a sharp exothermic peak followed by a small endothermic one for each injection (compare with Figure 1B). Note, however, that the magnitude of the exothermic peak is more than 10 times larger than that of simple chitosan dilution (Figure 1B). Figure 1E shows the integrated heats of binding as a function of the molar ratio of chitosan monomers to phospholipids in the external leaflet of the liposome membranes. The signal was corrected by subtracting the heat of chitosan dilution as measured in Figure 1B. The amount of accessible phospholipids located in the external membrane leaflet of the vesicles was calculated by taking into account the average diameter of the bare vesicles, as measured with DLS (see below), and a bilayer thickness of 5 nm.[27] Figure 1E shows that the binding of chitosan to neutral vesicles is exothermic and characterized by relatively weak molar enthalpy ΔH. The latter, as estimated from extrapolating the signal to zero molar ratios, is $\Delta H \cong -100$ cal/mol of chitosan monomer. Upon increasing molar ratios of chitosan monomers to lipids accessible for binding, the magnitude of the heat release diminishes as the vesicles become covered with chitosan and the number of free lipids decreases. The results for the binding heat imply that binding of positively ionized chitosan to the zwitterionic membrane of liposomes is characterized by a small exothermic enthalpy of interaction. The structure of the titration peaks in Figure 1C suggests that different forces and/or changes in structural properties of chitosan are involved in the process of chitosan binding to the vesicle membrane. Various types of behavior may be considered when chitosan comes in physical contact with liposomes, namely, change in the polymer conformation, changes in solvation of the polymer and the liposome membrane, electrostatic interactions, formation and breaking of hydrogen bonds, van der Waals forces, and polymer deionization. Hence, the molar enthalpy ΔH measured for this interaction may reflect the balance of different endothermic and exothermic contributions resulting from the sum of small heats of interaction.

It is interesting to note that a previous study of the interaction of DOPC vesicles with chitosan at pH 3.5 and 6.0 has shown it to be of endothermic nature,[14] contrary to what we observe here. However, the ITC measurements in ref 14 were performed in the presence of 200 mM sucrose solution. Having in mind the similarity in the chemical structure of sucrose and chitosan monomers, it could be expected that the sucrose–membrane interactions strongly influence the binding of chitosan to the membrane. It is known that, for example, sucrose solutions at this concentration dramatically change the bilayer properties, e.g., they decrease the bending stiffness of phosphocholine membranes.[28,29] Furthermore, in ref 14 the raw heat-flow data are not given, and thus, conclusions about various contributions of the heats of dilution cannot be made.

Even though the ITC signal in the explored range of molar ratios does not change significantly (see Figure 1), the ζ-potential and hydrodynamic diameter of the vesicles in the suspension
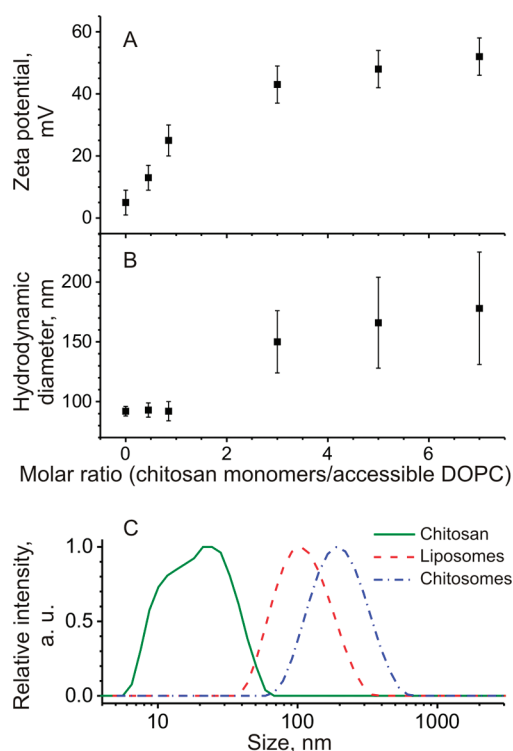
Figure 2. ζ-Potential (A) and dynamic light scattering data (B, C) for DOPC liposomes titrated with chitosan (25 °C). The data in panels A and B are shown as a function of chitosan monomers per DOPC present in the external leaflets of the vesicles. The error bars reflect the standard deviation. The normalized size distributions in (C) are for chitosan solution (solid curve), chitosan-free DOPC liposomes (dashed curve), and DOPC liposomes titrated with chitosan, corresponding to chitosan monomers/accessible DOPC 7:1 molar ratio (dash-dotted curve).

increase systematically with increasing chitosan concentration, as shown in Figure 2. Before titration, the liposomes are almost neutral (ζ-potential around 5 mV) with a diameter of around 92 nm. Below 1:1 stoichiometry of the monomeric chitosan to accessible lipid (i.e., lipid present only in the external vesicle leaflet), the vesicle size remains unchanged within the error of the measurement while the ζ-potential increases linearly with polymer concentration. The particle size increase is more pronounced when adding an excess of polymer (see Figure 2B, C), while the ζ-potential reaches a plateau for the higher concentrations. At excess chitosan concentration corresponding to seven chitosan monomers for each phospholipid of the external leaflet of the vesicles, the measured ζ-potential almost reaches the value for free chitosan in solution, which was measured to be 53 ± 7 mV. The DLS data also shows broadening of the size distributions, suggesting increased polydispersity of the vesicles. The observed size increase in the vesicle suspension could be due to polymer adsorption or vesicle aggregation, as discussed further.

Similar trends have been frequently reported in the literature,[15,20] indicating that chitosan effectively binds to the membrane of neutral vesicles. Figure 1E also shows that the binding continues throughout the whole range of explored molar ratios (the heat release decreases with each subsequent injection but does not reach zero). The exothermic signal suggests that binding of chitosan to the membrane stabilizes the polysaccharide and is energetically more favorable than dilution and diffusion in the solution. This is understandable considering that the low

solubility of chitosan characterized by critical aggregation concentration which is above 1.0 mg/mL in similar pH and buffer solutions[30] and that the solubilized chains tend to aggregate after a certain period of time.[31] Note that in our measurements the concentration of chitosan in the vesicle suspensions was always below the critical aggregation concentration of the polymer.

Another important result that may be pointed out here is that the reverse measurement, namely, titration of chitosan solution in vesicles suspension in the same concentration ranges, gives, on average, approximately the same results for the binding heat, hydrodynamic diameter, and ζ-potential as the titration of liposomes suspension in chitosan solution. Therefore, the method of mixing has no significant effect on the results obtained here.

3.2. Binding of Chitosan to Negatively Charged Liposomes. Biological membranes contain a large fraction of negatively charged lipids. To characterize the interaction of chitosan with such membranes we prepared negatively charged vesicles using mixtures of DOPC and DOPG at various molar fractions.

Figure 3A shows that the injection of chitosan in a suspension of liposomes containing as few as 10 mol % of DOPG produces relatively high exothermic signal compared to the results obtained with pure DOPC vesicles (compare Figure 3A,B with Figure 1D,E). With every following injection, the signal decreases as the net negative charge of the membrane becomes a little less negative, since it was partially neutralized by the chitosan chains adsorbed onto the vesicles with the previous injections. Hence, the energy release with the following injection is also a little lower and so on. For liposomes with 10% DOPG, the strong exothermic signal decays significantly after the first tree injections. Increasing the fraction of DOPG to 20, 30, and 40% systematically raises the number of exothermic (downward pointing) peaks to higher chitosan/phospholipid molar ratios, while the overall magnitude of the peaks is also higher for the vesicles with more DOPG (see Figure 3C,E,G). The corresponding integrated heats of binding as a function of the molar ratio of monomeric chitosan to accessible lipid are given in Figure 3B,D, F,H. The data were corrected for dilution effects by subtracting the signal from chitosan-in-buffer titration measured separately. In the different measurements, we find that the chitosan—lipid molar ratios, at which the signal has strongly decayed, correspond very well to 1:1 chitosan monomers to PG lipids present in the external leaflet of the vesicles (note that the horizontal axes in Figure 3B,D,F,H represents the molar ratio of chitosan monomers to total lipid in the external vesicle leaflet and not to accessible PG only). This suggests that the chitosan—PG binding process saturates when each PG lipid present at the outer leaflets of the vesicle membrane is bound to a chitosan monomer; i.e., the negative charges in the PG headgroups are neutralized by the counterions of protonated amino groups of the polysaccharide. As we will see later, this conclusion will be confirmed by our analysis of the binding equilibrium. The relatively strong signal in these measurements is indicative for an energetically favorable effective electrostatic interaction between the positively ionized amino groups of the solubilized chitosan and the negative charges at the polar heads of DOPG. Since the effect is highly exothermic, the ITC measurements allow for characterizing the binding equilibrium and determining the enthalpy associated with the electrostatic binding of chitosan to the liposome membrane, as discussed in the next section.

3.3. Thermodynamic Characterization of Chitosan Binding. The thermodynamic parameters of chitosan binding to the membrane of small liposomes were obtained from the ITC
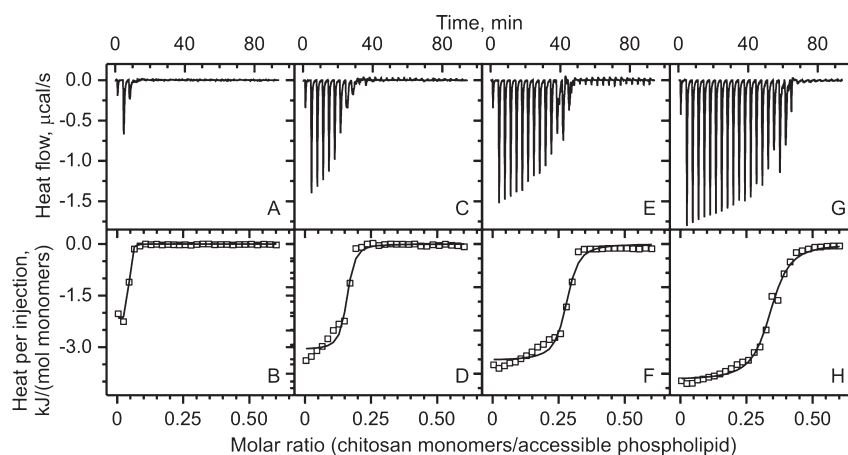
Figure 3. ITC data for the titration of chitosan (6.13 mM of monomers) into DOPC/DOPG liposomes (3.82 mM of total phospholipids) in a 80 mM acetate buffer at pH 4.48 (25 °C). The heat flow (A, C, E, G) and the respective integrated binding heat corrected for chitosan dilution (B, D, F, H) are plotted for vesicles with various molar fractions of DOPG: 10% (A, B), 20% (C, D), 30% (E, F), and 40% (G, H). The solid curves in panels B, D, F, and H are fits according to the model for one set of binding sites (see the text for details and Table 1 for the corresponding fitting parameters).

experiments by applying the model for a single set of identical binding sites as previously described by Ma et al. and employed for the characterization of chitosan binding to DNA.[32] The analysis was performed with a nonlinear least-squares fitting using the Origin software.[33] The model essentially describes the equilibrium between the free species of unbound lipids at the vesicle outer leaflet and unbound chitosan, whose concentration is introduced as chitosan monomers, and the bound chitosan monomers:

free binding site on the vesicle

$$+ \text{ free chitosan monomers} \rightleftarrows \text{bound chitosan monomers} \tag{1}$$
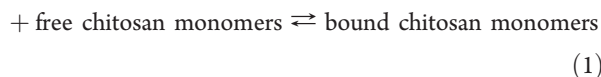
The binding constant, K, characterizing the equilibrium between the chitosan monomers and phospholipids from the external leaflet, is defined as

$$K = \frac{\Theta}{(1-\Theta)C_{ch}^{free}} \tag{2}$$

where $\Theta = [\text{bound chitosan}]/N[\text{L}]$ and is the fraction of lipids (the binding sites) occupied by chitosan monomers, $[\text{L}]$ is the total concentration of accessible lipid, and the number of binding sites N represents the number of chitosan monomers bound to each lipid at saturation of the binding sites. In eq 2, C_{ch}^{free} is the concentration of free chitosan (in moles monomers per liter), which can be expressed as

$$C_{ch}^{free} = C_{ch}^{tot} - N\Theta[\text{L}] \tag{3}$$

where C_{ch}^{tot} is the total monomeric chitosan concentration. Combining relations 2 and 3 gives a quadratic equation for the molar fraction Θ. Solving this equation provides an expression for Θ as a function of the lipid concentration.[32,33] Then, the heat release per injection, δQ, where the bound fraction changes by $\delta\Theta$, is $\delta Q = N[\text{L}]V\Delta H\delta\Theta$. Here V is the volume in the sample cell and ΔH is the molar enthalpy of process 1. Fitting the experimentally measured heat release δQ with this expression (see curves in Figure 3B,D,F,H) provides the fitting parameters N, K, and ΔH (for more details see refs 32, 33). From the equilibrium constant K one can then obtain the Gibbs free energy

of the process using $\Delta G = -RT\ln(55.55K)$, where ΔG is defined for standard state of mole fractions, T is temperature, and the factor 55.55 introduces the concentration of water. The entropy gain can then be estimated from the Gibbs free energy via $T\Delta S = \Delta H - \Delta G$.

Using the single set binding sites model we were able to fit very well the ITC data, as demonstrated in Figure 3B,D,F,H. The fitting parameters together with the calculated Gibbs free energy and the entropy gain are given in Table 1. Below we discuss the results for each of the thermodynamic parameters obtained with these analyses. Let us note that the model described above does not explicitly distinguish between binding of chitosan to PC and PG headgroups. The membrane is viewed as a homogeneous matrix, and the obtained parameters are effective. We refrained from distinguishing the specific interaction of chitosan with PG and PC separately because this would involve fitting with twice as many parameters, which is futile.

Comparing the values for the number of binding sites N obtained for suspensions of vesicles with various compositions, we find that this number increases with the PG fraction. This increase is linear (see Figure 4). Indeed, the proportionality factor of this dependence is 1; i.e., one chitosan monomer binds to one PG lipid at saturation of the binding sites, as speculated above. This is a reasonable result having in mind that the interaction of PG headgroups with the chitosan monomers produces the stronger binding compared to that with the PC headgroups. Since N is the number of chitosan monomers bound to each lipid at saturation, $1/N$ provides the ratio of accessible lipids to bound chitosan monomers at saturation. The dependence of $1/N$ as a function of PG content in the membrane is given in Figure 4B. It suggests that increasing the fraction of PG above around 30% does not lead to significantly decreasing the number of lipids per bound chitosan monomer beyond around 3. Presumably, this limitation results from the relatively large linear dimension of the chitosan monomer, which indeed is comparable to the area occupied by few lipids. In the following sections we will discuss the implications of this behavior.

We now consider the results obtained for the molar enthalpy ΔH. The fitting function for the heat release is a sigmoidal curve whose intercept with the vertical axis gives the value of the molar enthalpy. This is so because during the first injections every

Table 1. Effective Thermodynamic Parameters Characterizing the Interaction between Chitosan and PG-Doped Vesicles (ΔH, ΔG, and $T\Delta S$ are defined per mole of chitosan monomers)

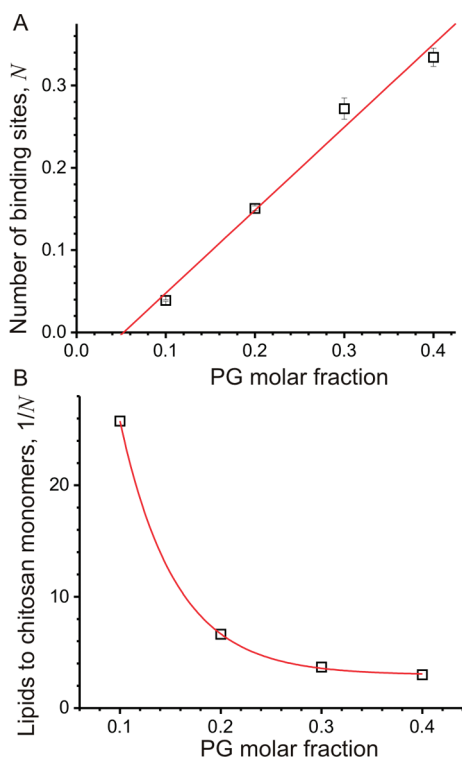| PG fraction (mol %)	number of binding sites, N	binding constant, K (10^5 M^{-1})	molar enthalpy, ΔH (kJ/mol)	Gibbs free energy, ΔG (kJ/mol)	entropic contribution, $T\Delta S$ (kJ/mol)
10	0.039 ± 0.001	14.27 ± 9.28	-2.19 ± 0.01	-45.08	42.90
20	0.151 ± 0.003	3.33 ± 1.12	-3.07 ± 0.02	-41.48	38.41
30	0.272 ± 0.013	2.47 ± 0.61	-2.70 ± 0.05	-40.74	38.03
40	0.334 ± 0.011	1.24 ± 0.70	-3.95 ± 0.05	-39.03	35.08

Figure 4. Dependence of the number of binding sites N at saturation (A) and the respective ratio of accessible lipids per bound chitosan monomer, $1/N$, at saturation (B) as a function of the PG fraction in the vesicle membrane. The error bars in part A are standard deviations as given in Table 1 and the red line is a linear fit with slope 1.0077 ± 0.09189. The curve in part B is an exponential decay fit guiding the eye.

added chitosan binds to bare or chitosan-free vesicles, while with increasing chitosan–lipid molar ratios, i.e., with every following injection, the membrane gradually becomes covered with chitosan, thus weakening the interaction with the free polymer. The values of ΔH obtained for the vesicles with 10 and 20% PG are less reliable because for these two measurements the initial plateau defining the intercept is less pronounced. Furthermore, the initial injection of 2 μL is usually ignored because of possible dilution in the preequilibration stage of the measurement. The corresponding value of ΔH characterizing the interaction of chitosan with the pure PC vesicles is on the order of -0.4 kJ/mol (see Figure 1E) and is thus much smaller than that obtained for the PG-doped vesicles.

The strong negative Gibbs free energy ΔG (see Table 1) calculated from the binding constant K shows that the electrostatic binding of chitosan is energetically favorable, leading to stabilization of the vesicle suspensions. Similar tendency has

been previously observed in the evaluation of the chemical shift anisotropy changes of the phosphate group of phospholipids in the presence of chitosan on the membrane of reverse-phase liposomes.[15]

The binding constant K is larger for the vesicles with smaller fraction of PG (see Table 1). This implies that the binding strength as characterized by the Gibbs free energy ΔG decreases with increasing PG fraction. A naïve explanation for this behavior could be steric hindrance resulting from the relatively large linear dimension of the chitosan monomer compared to the small spacing between the PG headgroups on the membrane at high concentration of PG. Such steric hindrance could also have implications on the way the whole polymer adsorbs on the membrane.

The entropy contribution obtained from ΔG and the measured molar enthalpy are given in Table 1. From the estimated values for ΔG and $T\Delta S$, it is obvious that the entropic contribution to the Gibbs free energy is significant for all types of studied membranes. Presumably, this large entropy gain arises from the release of water molecules. We could have considered entropic contributions as a source for the behavior of the binding constant as a function of the vesicle surface charge, as discussed in the previous paragraph. However, as demonstrated by the values of $T\Delta S$ in Table 1, this entropic contribution decreases for the highly charged membranes.

Overall, the enthalpy variation in all measurements shows strong exothermic binding between chitosan and the membrane of small liposomes when the electrostatic interaction is the main driving force. Compared to the isotherms obtained for neutral liposomes, as discussed in section 3.1, for the PG-doped membranes one may assume that the heat contributions from changes in chitosan conformation, solvation, hydrophobic interactions, hydrogen bonding, and deionization of amino groups have a relatively small influence.[32] Nevertheless, the significant entropy change we measure may result from some of these events but also from deionization, release of water molecules, changes in water structure, and alteration in ion distribution, as a consequence of the binding process mainly promoted by electrostatic interactions, as emphasized in previous studies.[32]

3.4. Chitosan-Mediated Aggregation of Liposomes. It is known that negatively charged liposomes may produce aggregates in the presence of chitosan.[20] In fact, most of the samples studied here have shown aggregation after completing the titration. This is evidenced by DLS measurements on the samples before and after the titration experiment. However, the neutral vesicles and the 10% DOPG vesicles have shown no aggregation or at least aggregation to a much lesser extent compared to the 20, 30, and 40% DOPG samples. This result suggests that the factors responsible for aggregation could be both the membrane charge and the chitosan concentration. To find out the approximate

Table 2. Results for the Hydrodynamic Diameter and the ζ-Potential (25 °C) for DOPC and DOPC/DOPG Liposomes (3.82 mM total phospholipids in 80 mM acetate buffer, pH 4.48) before and after Titration with Chitosan Solution (6.13 mM monomers concentration in 80 mM acetate buffer, pH 4.48)[a]

	before titration		after titration with chitosan		
DOPG fraction (mol %)	particle size (nm)	ζ-potential ($\pm$6 mV)	particle size (nm)	ζ-potential ($\pm$6 mV)	chitosan monomers/lipid
0	92 ± 6	5	122 ± 37	41	0.56
10	95 ± 5	−27	217 ± 25	43	0.56
20	101 ± 5	−51	404 ± 168	3	0.17
30	106 ± 6	−68	>1000	−14 (51%), 25 (49%)[b]	0.25
40	106 ± 8	−80	>1000	−57	0.32

[a] The data given for the 20, 30, and 40% PG vesicles correspond to the point where aggregation is first observed. The molar ratio of chitosan monomers to accessible lipid at which the data were collected is indicated in the last column. [b] The two values for the ζ-potential for the vesicles with 30% PG correspond to the two peaks detected in the ζ-potential distribution. The values in the parentheses reflect the area fraction of each peak.

chitosan concentration at which the aggregation takes place, we performed a separate experiment simulating the mixing process of chitosan solution into the vesicle suspension during an ITC measurement. Aliquots of 10 μL of chitosan solution were dropped stepwise in the vesicle suspension under continuous stirring. The size and the ζ-potential were measured after equilibration of about 5 min after adding the chitosan solution. The experiment was terminated after detecting significant aggregation in the sample except for the pure DOPC and the 10% PG vesicles (see Table 2). As exemplified for the 30% DOPG sample in Figure 5, micrometer-sized aggregates appear after reaching a concentration of 0.0768 mg/mL chitosan in the vesicles suspension, corresponding to a ratio of close to 0.24 monomers per accessible phospholipids. This result also shows that for a fixed PG fraction in the membrane, aggregates are formed above a certain concentration of chitosan. The ζ-potential reaches approximately its maximal value when aggregation is detected (data not shown).

The molar ratios of chitosan monomers to accessible lipid, above which aggregation is detected for the vesicles with 20, 30 and 40% PG (see Table 2), correspond also to the molar ratios, at which a significant decay in the ITC titration curves is observed (see Figure 3). As shown in the analyses in section 3.3, these ratios reflect the point at which the vesicles surface saturates with adsorbed chitosan. Thus, this saturation surface coverage (reflected by the fitting parameter N; see section 3.3) is achieved before vesicle aggregation is initiated, suggesting that the capacity of chitosan coverage on the membrane is relatively low in this production method, at least for the strongly negatively charged liposomes if one aims to avoid aggregation.

In the absence of chitosan, the ζ-potential of the vesicles naturally becomes more negative with increasing the PG fraction in the membrane (see Table 2). Their hydrodynamic diameter does not vary significantly and is around 100 nm. The vesicle suspensions show narrow distributions irrespectively of the PG content (data not shown). Similar results were found after titration of the vesicles with chitosan-free buffer. This indicates that the mechanical energy of titration has no effect on the vesicle characteristics.

After titration with the chitosan solution, different results were obtained depending on the concentration of DOPG. Vesicles containing 10 mol % of DOPG show an increase in size and ζ-potential, similar to the behavior of the neutral DOPC vesicles. Note that their zeta potential increases from −27 to 43 mV. Both for the pure DOPC vesicles and those with the 10% PG, the size
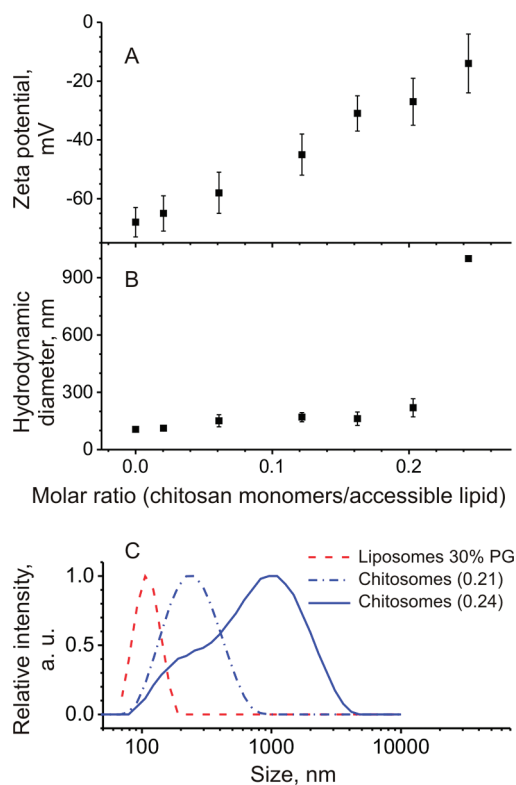

Figure 5. ζ-Potential (A) and dynamic light scattering data (B, C) for 30% DOPG liposomes titrated with chitosan (25 °C). The data in parts A and B are shown as a function of chitosan monomers per lipid present in the external leaflets of the vesicles. The error bars correspond to standard deviation. Note that the last data point in part B has no variation due to the very broad size distribution as a result of aggregation; see the solid curve in part C. The normalized size distributions in part C are for 30% DOPG liposomes (solid curve) and the same liposomes titrated with chitosan corresponding to molar ratios of chitosan monomers to accessible lipid of 0.21 and 0.24 (dashed and dashed−dotted curves, respectively).

increase most probably results from the adsorption of chitosan on the vesicles (see also Figure 2C). Note that the size of the polymer as measured with DLS is approximately 39 ± 21 nm. On the other hand, vesicles with higher DOPG concentration show aggregation (see also Figure 5C). Their ζ-potential increases to neutrality for the suspension with 20% PG, it is bimodal for the
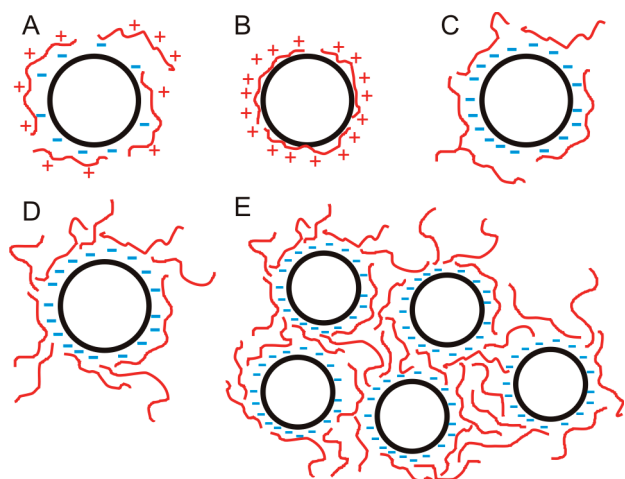
Figure 6. Schematic representations of chitosome structures: (A) The positive chains of chitosan are attracted by the negative charges at the surface of a small liposome. (B) The chitosan chains tightly cover the external leaflet of the membrane of a neutral or slightly negative liposome; the negative charges are neutralized and the external surface charge turns positive. (C) The chitosan chains are attracted by a small liposome with a strong negative surface charge. (D) At higher concentration, the chitosan chains bind to the remaining free spaces on the external leaflet of a strongly negative liposome. (E) Aggregates of chitosomes form above a certain concentration of chitosan chains; the net surface charge remains negative, showing that aggregation is not related to charge reversal (see the text for details).

30% (positive and negative peaks), and it remains strongly negative for the 40% DOPG, despite the substantial increase from −80 to −57 mV. These results have considerable importance, since they evidence that saturation of chitosan on the liposome membrane and vesicle aggregation are not necessarily related to charge reversal. We speculate that the strength of chitosan adsorption on the membrane must play a crucial role in the organization of the polymer chains on the vesicles. Supported by the experimental results reported herein, we propose a model to explain the behavior of the system, as shown in Figure 6 and discussed in the following section.

3.5. Chitosome Structure. As a starting point, we consider the dimensions of the liposomes and the chitosan chains. The vesicles are spherical with a diameter of around 100 nm. They have narrow size distribution because of the exhaustive repetition of the extrusions during preparation and show high efficiency for size standardization. Chitosan is a linear polysaccharide, and the polymer chains are extended when the amino groups are ionized in a good solvent. Solubilized chitosan typically adopts the structure of a flexible rodlike macromolecule with persistence length between 6 and 22 nm,[34] as shown by TEM images (see, for example, ref 35). The size of the extended chains depends largely on the molecular weight of the polymer. For the chitosan employed here, we have obtained a hydrodynamic radius of 39 nm with a radius of gyration around 46 nm. The large size variation denotes the wide molecular weight distribution (see Figure 2C), an inherent characteristic of the polysaccharide. The ratio between the radius of gyration and the hydrodynamic radius, also known as the ρ-parameter, is 1.2, confirming the flexible chainlike structure of the polymer.[36] Thus, the DLS measurements show that small liposomes and chitosan have similar dimensions, despite the spherical shape of the former and the linear-rod structure of the latter.

Having in mind these arguments one could speculate that, upon binding of chitosan to the surface of a small vesicle, the polymer chain bends to adapt to the large curvature of the sphere, as represented in Figure 6A. For the weakly charged membrane, the binding strength is larger (as exemplified by the estimates for values of the Gibbs free energy in Table 1), which could provide energy for bending conformation of the polymer during the adsorption on the membrane. For the neutral and slightly negatively charged liposomes (10% DOPG) the range of electrostatic attraction is short and they only weakly attract the polymers, allowing the chitosan chains more "time" to bend and better organize over the membrane (Figure 6A). With increasing concentration of chitosan on the membrane, the negative charges are neutralized and the net charge of the membrane turns highly positive (Figure 6B). The vesicles start to repel each other; therefore, aggregation is avoided (see Figure 2C and Table 2). The DLS data indicating a weak increase in the vesicle radius also suggest relatively flat adsorption of the polymer over the membrane of neutral or slightly negatively charged vesicles, confirming similar behavior reported in earlier studies.[20] Furthermore, from a morphological viewpoint, atomic force microscopy studies have shown that chitosan incorporation in phospholipid monolayers leads to a considerable increase in the thickness but also in the roughness of the film.[18]

As demonstrated in our analyses of the ITC data, the binding strength decreases with increasing fractions of PG. Thus, the long polymer chains may not completely adsorb flatly on the highly charged vesicle surface, as discussed below. Indeed, above a certain coverage of the membrane by the chains that are already adsorbed, the newly injected polymer chains will have to bind to the free spaces on the membrane, but these free spaces may not be large enough for adsorption of the complete chains. Apart from this steric hindrance, the newly injected chains will avoid overlapping with other chains already adsorbed due to electrostatic repulsion and excessive restructuring of the hydration water. Thus, the organization of chitosan on the membrane may be poorer, since the presence of loops may hinder the adsorption of the new chains. Such behavior has been previously reported whereby chitosan has shown segment−segment interaction on the surface of strongly negatively charged mica.[37]

As mentioned before, the positively ionized amino groups of chitosan are attracted by the negative charges on the vesicle membrane. The larger such negative charge is, the longer the range of the attraction between both structures will be, and thus the local concentration of chitosan in the vicinity of a vesicle will be higher. At the same time, the capacity of the vesicles to adsorb chitosan monomers increases with the fraction of PG. This is demonstrated by the higher chitosan/lipid molar ratios at which the signal in the ITC measurement decays (see Figure 3) and by the respective number of binding sites N, as determined by the fitting. Thus, the more charged membranes are able to bind a higher concentration of chitosan, as shown by the ITC results in Figure 3 when increasing the DOPG content.

Having in mind the above consideration, the following picture for the adsorption of chitosan on the highly charged vesicle emerges. As sketched in Figure 6C, the chitosan chains are strongly attracted to the membrane, but as a result of the weaker binding strength, the organization of the polymer over the membrane is lower than for the neutral and 10% PG vesicles. Above a certain surface concentration of chitosan, where the net charge still remains negative as shown by the ζ-potential, the newly added chitosan is still attracted to the vesicles, but now the

chains do not bind flatly but adsorb partially to the remaining spots free for binding (Figure 6D). Because of the lower organization over the membrane, the partially bound chains may build bridges to neighboring vesicles, inducing aggregation (Figure 6E). However in this case, the net ζ-potential still remains negative (Table 2), indicating that the amount of chitosan was not sufficient to neutralize all the charges on the highly charged membranes (30 and 40% PG). Therefore, the strength of chitosan adsorption on the liposome membrane is presumably the main reason for aggregation before charge reversal. Indeed, as also pointed out by Pavinatto et al.,[17] the surface potential of the phospholipid membrane as well as the conformation of the polysaccharide chains are both responsible for the final morphology and characteristics of the chitosan-decorated membrane.

4. SUMMARY AND CONCLUDING REMARKS

The heat release observed for the interaction of chitosan with small zwitterionic liposomes is not surprising considering that the positively ionized amino groups of chitosan tend to remain protonated in the absence of counterions. Similar results have been described for the interaction of chitosan with whey protein at pH 5.[38] Nevertheless, chitosan also adsorbs to neutral membranes, suggesting the involvement of other forces besides electrostatics. The binding can be interpreted for instance as a result of reduction of the electrostatic repulsion between the protons in acidic solution and the positive amino groups of the chitosan chains. In this way the state of lower free energy corresponds to the situation where chitosan is adsorbed to the liposomes and thus the binding releases some energy. However, when the extended linear chains come in physical contact with the colloidal structures with similar dimensions, they have to bend in order to adapt to the high curvature of the vesicle membrane, and this consumes energy. On the other hand, entropic contributions possibly due to water rearrangement like liberation of hydration water are also in favor of the adsorption process. The resulting energy released from the sum of the various contributions is small but still enough to promote polymer binding.

The strength of chitosan adsorption is also influenced by the membrane surface charge. As evidenced by the results for the Gibbs free energy characterizing the polymer adsorption to PG-doped vesicles, the higher the net negative charge, the weaker the binding is, leading to weaker chain organization over the membrane. At the saturation point, aggregation of structures takes place and it has been shown that this behavior is not always related to charge reversal. Rather, the strongly negative surface charge can influence the structures in a manner that some loose segments of the polymer chains may be attracted by the charges of neighboring vesicles, leading to liposome aggregation. Here, we did not perform studies employing positively charged lipids because these are not naturally occurring in cells. However, research in this direction is worth being pursued, since the variety of lipids previously employed in chitosome formation is still very limited and needs to be expanded if successful drug delivery applications are sought for.

■ AUTHOR INFORMATION

Corresponding Authors
*(O.M.) E-mail: Omar.Mertins@mpikg.mpg.de. (R.D.) E-mail: Rumiana.Dimova@mpikg.mpg.de. Tel: +49 3315679615. Fax: +49 3315679612.

■ REFERENCES

(1) Bangham, A. D.; Standish, M. M.; Watkins, J. C. Diffusion of univalent ions across lamellae of swollen phospholipids. *J. Mol. Biol.* **1965**, *13* (1), 238.

(2) Lasic, D. D., *Liposomes: From Physics to Applications*; Elsevier: Amsterdam, 1993.

(3) Lasic, D. D. Novel applications of liposomes. *Trends Biotechnol.* **1998**, *16* (7), 307–321.

(4) Drummond, D. C.; Meyer, O.; Hong, K. L.; Kirpotin, D. B.; Papahadjopoulos, D. Optimizing liposomes for delivery of chemotherapeutic agents to solid tumors. *Pharmacol. Rev.* **1999**, *51* (4), 691–743.

(5) Mima, S.; Miya, M.; Iwamoto, R.; Yoshikawa, S. Highly deacetylated chitosan and its properties. *J. Appl. Polym. Sci.* **1983**, *28* (6), 1909–1917.

(6) Takeuchi, H.; Matsui, Y.; Sugihara, H.; Yamamoto, H.; Kawashima, Y. Effectiveness of submicron-sized, chitosan-coated liposomes in oral administration of peptide drugs. *Int. J. Pharm.* **2005**, *303* (1–2), 160–170.

(7) Maron, L. B.; Covas, C. P.; Da Silveira, N. P.; Pohlmann, A.; Mertins, O.; Tatsuo, L. N.; Sant'Anna, O. A. B.; Moro, A. M.; Takata, C. S.; De Araujo, P. S.; Da Costa, M. H. B. LUVs recovered with chitosan: A new preparation for vaccine delivery. *J. Liposome Res.* **2007**, *17* (3–4), 155–163.

(8) Campana Filho, S. P.; Desbrières, J., Chitin, chitosan and derivatives. In *Natural Polymers and Agrofibers Based Composites*; Suprema Gráfica: São Carlos, 2000; pp 41–71.

(9) Mertins, O.; Sebben, M.; Pohlmann, A. R.; da Silveira, N. P. Production of soybean phosphatidylcholine–chitosan nanovesicles by reverse phase evaporation: A step by step study. *Chem. Phys. Lipids* **2005**, *138* (1–2), 29–37.

(10) Mertins, O.; Cardoso, M. B.; Pohlmann, A. R.; da Silveira, N. P. Structural evaluation of phospholipidic nanovesicles containing small amounts of chitosan. *J. Nanosci. Nanotechnol.* **2006**, *6* (8), 2425–2431.

(11) Lionzo, M.; Mertins, O.; Pohlmann, A. R.; da Silveira, N. P. Phospholipid/chitosan self-assemblies analyzed by SAXS and light scattering. *Synchrotron Radiat. Mater. Sci.* **2009**, *1092*, 127–129.

(12) Mertins, O.; Lionzo, M. I. Z.; Micheletto, Y. M. S.; Pohlmann, A. R.; da Silveira, N. P. Chitosan effect on the mesophase behavior of phosphatidylcholine supramolecular systems. *Mater. Sci. Eng., C* **2009**, *29* (2), 463–469.

(13) Mertins, O.; da Silveira, N. P.; Pohlmann, A. R.; Schroder, A. P.; Marques, C. M. Electroformation of giant vesicles from an inverse phase precursor. *Biophys. J.* **2009**, *96* (7), 2719–2726.

(14) Quemeneur, F.; Rinaudo, M.; Maret, G.; Pepin-Donat, B. Decoration of lipid vesicles by polyelectrolytes: Mechanism and structure. *Soft Matter* **2010**, *6* (18), 4471–4481.

(15) Mertins, O.; Schneider, P. H.; Pohlmann, A. R.; da Silveira, N. P. Interaction between phospholipids bilayer and chitosan in liposomes investigated by P-31 NMR spectroscopy. *Colloids Surf., B* **2010**, *75* (1), 294–299.

(16) Fang, N.; Chan, V.; Mao, H. Q.; Leong, K. W. Interactions of phospholipid bilayer with chitosan: effect of molecular weight and pH. *Biomacromolecules* **2001**, *2* (4), 1161–1168.

(17) Pavinatto, A.; Pavinatto, F. J.; Barros-Timmons, A.; Oliveira, O. N. Electrostatic interactions are not sufficient to account for chitosan bioactivity. *ACS Appl. Mater. Interfaces* **2010**, *2* (1), 246–251.

(18) Pavinatto, F. J.; Caseli, L.; Pavinatto, A.; dos Santos, D. S.; Nobre, T. M.; Zaniquelli, M. E. D.; Silva, H. S.; Miranda, P. B.; de Oliveira, O. N. Probing chitosan and phospholipid interactions using

Langmuir and Langmuir—Blodgett films as cell membrane models. *Langmuir* **2007**, *23* (14), 7666–7671.

(19) Pavinatto, F. J.; Pacholatti, C. P.; Montanha, E. A.; Caseli, L.; Silva, H. S.; Miranda, P. B.; Viitala, T.; Oliveira, O. N. Cholesterol mediates chitosan activity on phospholipid monolayers and Langmuir—Blodgett films. *Langmuir* **2009**, *25* (17), 10051–10061.

(20) Henriksen, I.; Smistad, G.; Karlsen, J. Interactions between liposomes and chitosan. *Int. J. Pharm.* **1994**, *101* (3), 227–236.

(21) Quemeneur, F.; Rinaudo, M.; Pepin-Donat, B. Influence of molecular weight and pH on adsorption of chitosan at the surface of large and giant vesicles. *Biomacromolecules* **2008**, *9* (1), 396–402.

(22) Laye, C.; McClements, D. J.; Weiss, J. Formation of biopolymer-coated liposomes by electrostatic deposition of chitosan. *J. Food Sci.* **2008**, *73* (5), N7–N15.

(23) Mady, M. M.; Darwish, M. M.; Khalil, S.; Khalil, W. M. Biophysical studies on chitosan-coated liposomes. *Eur. Biophys. J.* **2009**, *38* (8), 1127–1133.

(24) Godderz, L. J.; Peak, M. M.; Rodgers, K. K. Analysis of biological macromolecular assemblies using static light scattering methods. *Curr. Org. Chem.* **2005**, *9* (9), 899–908.

(25) MacDonald, R. C.; MacDonald, R. I.; Menco, B. P. M.; Takeshita, K.; Subbarao, N. K.; Hu, L. R. Small-volume extrusion apparatus for preparation of large, unilamellar vesicles. *Biochim. Biophys. Acta* **1991**, *1061* (2), 297–303.

(26) Pereira-Lachataignerais, J.; Pons, R.; Panizza, P.; Courbin, L.; Rouch, J.; Lopez, O. Study and formation of vesicle systems with low polydispersity index by ultrasound method. *Chem. Phys. Lipids* **2006**, *140* (1−2), 88–97.

(27) Petrache, H. I.; Tristram-Nagle, S.; Gawrisch, K.; Harries, D.; Parsegian, V. A.; Nagle, J. F. Structure and fluctuations of charged phosphatidylserine bilayers in the absence of salt. *Biophys. J.* **2004**, *86* (3), 1574–1586.

(28) Genova, J.; Zheliaskova, A.; Mitov, M. D. The influence of sucrose on the elasticity of SOPC lipid membrane studied by the analysis of thermally induced shape fluctuations. *Colloids Surf., A* **2006**, *282*, 420–422.

(29) Vitkova, V.; Genova, J.; Mitov, M. D.; Bivas, I. Sugars in the aqueous phase change the mechanical properties of lipid mono- and bilayers. *Mol. Cryst. Liq. Cryst.* **2006**, *449*, 95–106.

(30) Philippova, O. E.; Volkov, E. V.; Sitnikova, N. L.; Khokhlov, A. R.; Desbrieres, J.; Rinaudo, M. Two types of hydrophobic aggregates in aqueous solutions of chitosan and its hydrophobic derivative. *Biomacromolecules* **2001**, *2* (2), 483–490.

(31) Kjoniksen, A. L.; Iversen, C.; Nystrom, B.; Nakken, T.; Palmgren, O. Light scattering study of semidilute aqueous systems of chitosan and hydrophobically modified chitosans. *Macromolecules* **1998**, *31* (23), 8142–8148.

(32) Ma, P. L.; Lavertu, M.; Winnik, F. M.; Buschmann, M. D. New Insights into chitosan—DNA interactions using isothermal titration microcalorimetry. *Biomacromolecules* **2009**, *10* (6), 1490–1499.

(33) ITC data analysis in Origin. In *Tutorial Guide*, 7th ed.; MicroCal LLC: Northampton, MA, 2004.

(34) Berth, G.; Dautzenberg, H.; Peter, M. G. Physico-chemical characterization of chitosans varying in degree of acetylation. *Carbohydr. Polym.* **1998**, *36* (2−3), 205–216.

(35) Anthonsen, M. W.; Varum, K. M.; Hermansson, A. M.; Smidsrod, O.; Brant, D. A. Aggregates in acidic solutions of chitosans detected by static laser-light scattering. *Carbohydr. Polym.* **1994**, *25* (1), 13–23.

(36) Burchard, W. Solubility and solution structure of cellulose derivatives. *Cellulose* **2003**, *10* (3), 213–225.

(37) Claesson, P. M.; Ninham, B. W. pH-Dependent interactions between adsorbed chitosan layers. *Langmuir* **1992**, *8* (5), 1406–1412.

(38) de Souza, H. K. S.; Bai, G. Y.; Goncalves, M. P.; Bastos, M. Whey protein isolate—chitosan interactions: A calorimetric and spectroscopy study. *Thermochim. Acta* **2009**, *495* (1−2), 108–114.